Chaos, Solitons & Fractals 44 (2011) 122–130

Contents lists available at ScienceDirect

Chaos, Solitons & Fractals

Nonlinear Science, and Nonequilibrium and Complex Phenomena

journal homepage: www.elsevier.com/locate/chaos

Functional motifs: a novel perspective on burst synchronization and regularization of neurons coupled via delayed inhibitory synapses

Igor Franović, Vladimir Miljković *

Faculty of Physics, University of Belgrade, P.O. Box 44, 11001 Belgrade, Serbia

ARTICLE INFO

Article history:
Received 6 September 2010
Accepted 30 December 2010
Available online 15 February 2011

ABSTRACT

For one of the most common network motifs, an inhibitory neuron pair, we perform an extensive study of burst synchronization and the related phenomena applying the model of Rulkov maps coupled via delayed synapses. Instigated by the phase-plane analysis, that has the neuron switching between the noninteracting and the interacting map, it is demonstrated how the system evolution may be interpreted by means of the dynamical configurations of the motif, each represented by an extracted subgraph. Under the variation of the synaptic parameters, the probability of finding synchronized neurons in a given configuration is seen to reflect the way in which the anti-phase synchronization is eventually superseded by the synchronization in phase. Such an approach also provides a novel insight into regularization, characterizing the neuron bursting in either of these regimes. Looking into correlation of the two neurons' bursting cycles we acquire a deeper understanding of the more sophisticated mechanisms by which the regularity in the time series is maintained. Further, it is examined whether introducing heterogeneity in the neuron or the synaptic parameters may prove advantageous over the homogeneous case with respect to burst synchronization.

1. Introduction

Maintaining focus on local connectivity pathways, it has come to light that the complex networks are assembled from recurring blocks, network motifs [1–3], identified as being significatively over-represented in a given network when compared to an ensemble of equivalent random graphs. At present, there is a plethora of evidence in support of the argument that many of the large scale neural networks exhibit the properties of different types of complex networks, like small-world, scale free or hierarchical ones [4,5], and can indeed be classified into superfamilies by the distribution of triads and the other, higher order constituent motifs [1,2]. Mediated by such a structural skeleton [6–8], the neural networks demonstrate highly adaptive responses to variable stimuli and the flexibility in information processing. Due to a demand for a substantial degree of functional specialization, only a fraction of the available synaptic connections are recruited at a time, imposing a kind of dynamical, "effective" circuits on top of the physiological ones [9]. One is therefore led to distinguish between the structural and the functional motifs [6], where the latter refer to the possible combinations of links contained in the former, making up a set of subgraphs within the original motif's graph. Though a clear-cut relationship as to the likelihood of the appearance is yet to be established, their number and diversity seem to be ruled by an optimization principle [6,9], promoting a rich and diverse repertoire of functional motifs over a comparably smaller and more modest selection of the structural elements.

In terms of performing the operational tasks, much of the activity relies on synchronized outputs of the participant neurons [10], that often generate chaotic bursting patterns, as consistent with the findings in the CPGs [11,12] and several specific brain areas [13,14]. Synchronization

* Corresponding author. Tel.: +38 1112630152; fax: +38 1113282619.
E-mail addresses: igor.franovic@gmail.com (I. Franović), vladimir.miljkovic@ff.bg.ac.rs (V. Miljković).

0960-0779/$ - see front matter © 2011 Elsevier Ltd. All rights reserved.
doi:10.1016/j.chaos.2010.12.009

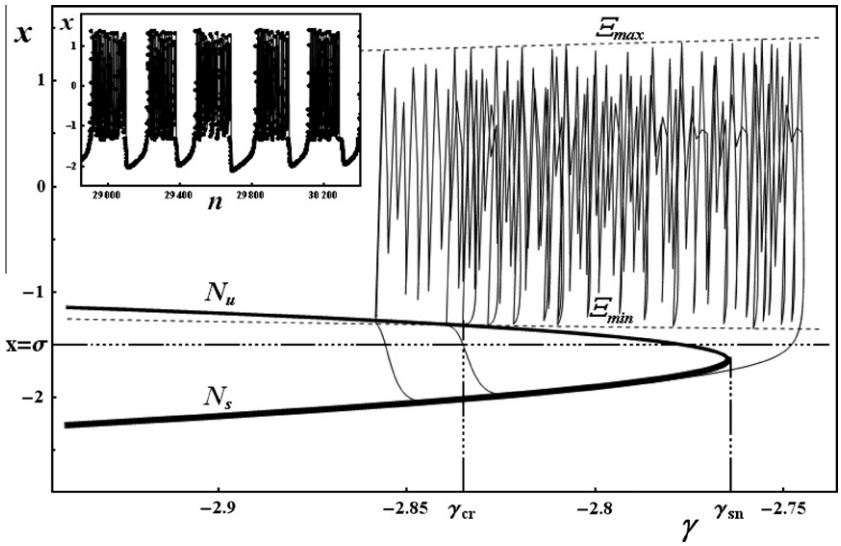

Fig. 1. Blowup of the bistability region of the fast subsystem. Bursting is enabled if the slow variable nullcline $x_n = \sigma$ intersects the branch of unstable fixed points N_u. γ increases (decreases) whenever the phase point lies below (above) the slow nullcline. Phase point climbing along the stable branch N_s coincides with the interburst intervals, whereas the bursts are approximately delimited by the points of the saddle-node bifurcation $\gamma = \gamma_{sn}$ and the external crisis $\gamma = \gamma_{cr}$. The irregularity in the series of an autonomous neuron comes from the termination of bursts being delayed beyond γ_{cr}. The inset displays a typical waveform, obtained for $\alpha = 4.15$ and $\sigma = -0.9$.

may then assume different forms [15–17], including individual spike synchronization, intermittent synchronization, complete (exact) synchronization and burst synchronization. Reflecting the notion of chaotic phase synchronization [18], under burst synchronization one would typically consider matching the respective times of onset and termination of bursts, refining its understanding further as required by the system at hand.

In an effort to unite the concepts laid out, we take as an exemplar one of the commonest structural motifs, an inhibitory neuron pair [7,8,19], aiming to highlight the role of the functional motifs, here alternatively termed dynamical configurations, viz. their contribution in the emergence and the succession of the synchronous rhythms with the variation of the synaptic parameters. This makes it important to revisit in a systematic way the well known claims on how the instantaneous synapses lead to antiphase synchronization [11,20], whereas the addition of the sufficient delay induces the synchronization in phase [19,21]. Another point to consider is the regularization of the burst cycles [22], exhibited by neurons in either of these regimes.

To provide such a perspective, it turns out extremely useful to employ the model of chaotic Rulkov maps [22,23], accompanied by a sufficiently detailed model of the delayed chemical synapses. Instigated by the phase plane analysis, presenting the neuron dynamics in terms of switches between the noninteracting and the interacting map [17], we monitor the probabilities of finding synchronized neurons in the allowed dynamical configurations, in effect determining how the particular functional motifs become promoted or inhibited by the variation of the synaptic weight and the transmission delay. This approach enabled us not only to understand the rationale behind the different synchronized regimes, but also to examine some of the more specific details, e.g. how come that there is an optimal weight range for achieving synchronization in phase, whose location gets shifted depending on the synaptic threshold behavior. Along with the insight stemming from quantifying the regularity of the burst cycle sequences, another gain lies in explaining why the neurons are prone to periodic bursting in view of the mechanisms driving their mutual adaptation. Closing the argument, we introduce a method to review the effects that the stimuli or weight heterogeneity may hold on burst synchronization.

2. Model and the applied methods

The study of the binary motif rests on the dynamics provided by the two-dimensional map

$$\begin{aligned} x_{i,n+1} &= \frac{\alpha}{1+x_{i,n}^2} + y_{i,n} - g_{c,ij}(x_{i,n}-v)\frac{1}{1+\exp(-k(x_{j,n-\tau}-\theta))}, \\ y_{i,n+1} &= y_{i,n} - \mu(x_{i,n}-\sigma), \end{aligned} \tag{1}$$

where n denotes the iteration step, and the indices $i, j \in \{1,2\}$ $(i \neq j)$ specify the post- and the presynaptic neuron, respectively. Without the interaction term, Eq. (1) reduces to the chaotic Rulkov model that, with the appropriate choice of parameters, yields square-wave bursts [22]. Setting $\mu = 0.001$, the neuron state is defined by the fast variable $x_{i,n}$ and the slow variable $y_{i,n}$, the former of which embodies the membrane potential, and the action of the latter is reminiscent of that of the gating variables. Consistent with the phenomenological nature of the model, some of the variables, such as α, make no reference to any physiological processes. In terms of the phase space structure, cf. [23,24], and the exhibited dynamical modes [17,25], it is indicated how among the conductance-based models

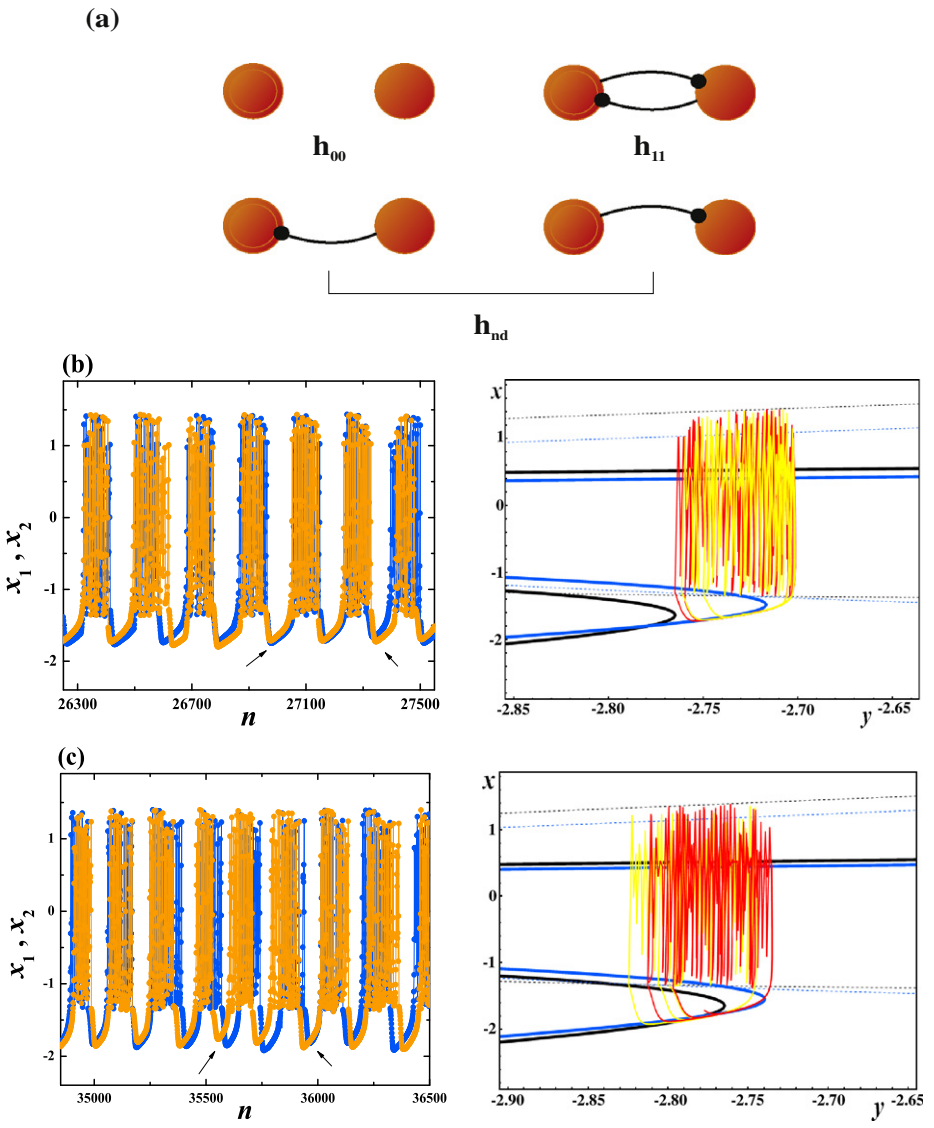

Fig. 2. (a) Subgraphs corresponding to the dynamical configurations of the inhibitory motif, designated by the h-quantities they contribute to. (b) Burst synchronization phenomena, quantified by the terms h_{00} and h_{11}, displayed together. On the left is the time series obtained for $g_c = 0.2$ and $\tau = 90$ showing the two neurons, coded blue (dark grey) and orange (light grey), synchronized in phase. The sequence between the arrows is extracted for the phase plane analysis on the right, that demonstrates how in this regime h_{00} and h_{11} may be viewed as complementary: the joint bursting occurs on the isolated map, whereas silence takes place on the interacting map. (c) The analysis analogous to the one in (b), carried out for the hnd term. The time series for $g_c = 0.12$ and $\tau = 60$ exhibit a form of burst synchronization where the two neurons lie on distinct maps. The sequence superimposed in the phase plane has the orange (light grey) neuron from the left bursting by the isolated, and the blue (dark grey) one by the interacting map. (For interpretation of the references to colour in this figure legend, the reader is referred to the web version of this article.)

the Hindmarsh–Rose neurons can be considered as the closest counterparts to the Rulkov ones. A brief summary of the ensuing analysis for the isolated neuron, treating $y_{i,n}$ as a control parameter γ within the fast subsystem, is presented in Fig. 1, and one may also address [17,23] for a comprehensive review. Here we only mention that the phase point motion is guided by the fast nullclines, merged in an S-curve, and the curves of minimal and maximal map iterates, Ξ_{min} and Ξ_{max}, providing the burst envelopes. As a key point, bursting dynamics relies on the existence of the bistability region in the fast subsystem that arises if $\alpha > 4$. Varying α can be used to control the irregularity of bursts: the closer α gets to 4, the less chaotic the bursting series becomes. Throughout the paper we select $\alpha = 4.15$ that provides a reasonable balance between the bursts' duration and the stochasticity associated with their termination delay [13,23]. Nonetheless, adjusting α to other values may evoke different forms of neuronal dynamics, including excitable behavior ($\alpha < 2$), periodic pulses or bursts ($2 < \alpha < 4$), as well as chaotic pulses for $\alpha > 4.6$ [26]. On the remaining intrinsic parameter σ, except when discussing the effects of stimulus inhomogeneity, the

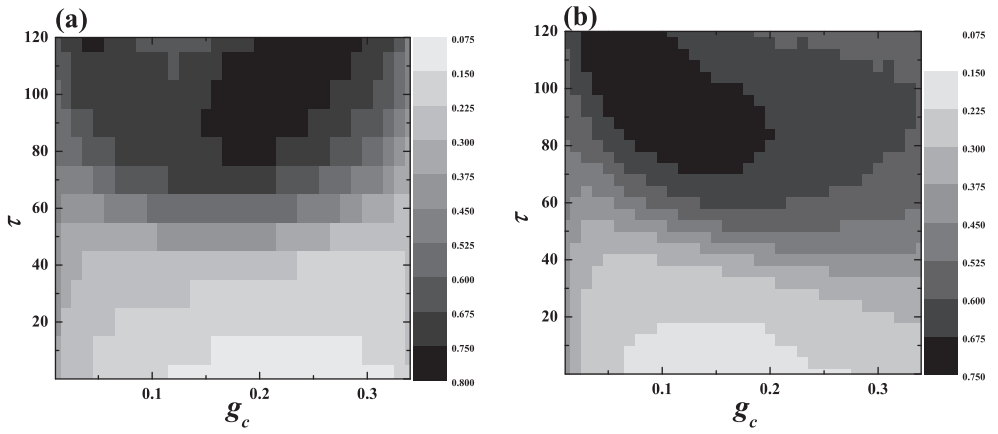

Fig. 3. Quantity H in the (g_c, τ) plane, plotted for the gain parameters $k = 25$ in (a) and $k = 5$ in (b). The higher values, distinguished by the darker shading, reflect how the increasing τ gives rise to burst synchronization. Displayed darkest is the domain of maximal synchronization (DMS), characterized by the genuine in-phase synchronization. Note that the change in synaptic threshold behavior is accompanied by the reverse orientation of the respective DMS.

external dc bias current is taken to be uniform, assuming the value $\sigma = -0.9$.

Moving onto the interaction term, the reversal potential [13] $v = -1.8$ is set so as to give the synapses the inhibitory character. Hereafter, the synaptic weights are assigned an equal value, $g_{c,ij} = g_c$, with the case of disparate weights discussed late in the paper. The time lag τ is reflected by the delayed arrival of the presynaptic potential influencing the gate opening. Within the sigmoid, for the activation threshold is chosen $\theta = -1.4$, a value easily reached by the bursting neuron. The sharpness of the synaptic response is determined by the gain parameter k [15,27,25]. The $k \gg 1$ case yields the fast threshold modulation model (FTM) [28], approximating well the action of the majority of chemical synapses in the brain [20,29], while for $k \sim 1$ one obtains the graded synaptic transmission model [30], suitable for describing the CPGs. For most of the paper we keep $k = 25$ fixed, though the value $k = 5$ will also be considered.

In the following we address the possibility of blending the phase plane approach into a framework seeking to characterize how the level of burst synchronization depends on the neuron and synaptic parameters. To this end, it is convenient to transform the time series of the interacting neurons' membrane potentials into symbolic sequences $\{S_{i,n}\}$. We apply a conversion rule T that ascribes $S_{i,n} = 1$ if the neuron is bursting, and -1 otherwise:

$$S_{i,n} = T(x_{i,n}) = \begin{cases} 1, & x_{i,n} \text{ in the bursting range;} \\ -1, & x_{i,n} \text{ in the silence range.} \end{cases} \quad (2)$$

The two ranges are distinguished by a useful rule of thumb stating that a neuron is bursting (silent) when its potential is above (below) θ. One of the advantages of the model lies in the opportunity to immediately relate the results coming from the phase plane analysis with the quantities applied to measure burst synchronization. The former reveal that, by including the interaction, the original neuron map gets shifted rightward and upward in the phase plane, maintaining the shape and the ensuing stability features of the curves of fixed points. In the previous article [17] we demonstrated how the neuron dynamics may be viewed in terms of switches between the isolated and the interacting map, a description that holds exactly in case of the fast threshold modulation ($k \gg 1$), where the synaptic states are defined as open/close, conforming to a Heaviside-like limit of the sigmoidal threshold function. In a way, the motif's effective structure is then dynamical by nature, contingent on the temporary openness of the synapses, with possibilities of neither, one or both of the synapses being open, see Fig. 2(a). With regard to these configurations of the motif, translated into maps guiding the individual neuron dynamics, we introduce a set of quantities, designated h_{00}, h_{11} and h_{nd}:

$$\begin{aligned} h_{00} &= \frac{1}{N_{max}} \left\langle \sum_{n=1}^{N_{max}} \delta_{S_{1,n},S_{2,n}} \Theta(\theta - x_{1,n-\tau}) \Theta(\theta - x_{2,n-\tau}) \right\rangle, \\ h_{11} &= \frac{1}{N_{max}} \left\langle \sum_{n=1}^{N_{max}} \delta_{S_{1,n},S_{2,n}} \Theta(x_{1,n-\tau} - \theta) \Theta(x_{2,n-\tau} - \theta) \right\rangle, \\ h_{nd} &= \frac{1}{N_{max}} \left\langle \sum_{n=1}^{N_{max}} \delta_{S_{1,n},S_{2,n}} (\Theta(x_{1,n-\tau} - \theta) \Theta(\theta - x_{2,n-\tau}) \right. \\ &\quad \left. + \Theta(\theta - x_{1,n-\tau}) \Theta(x_{2,n-\tau} - \theta)) \right\rangle, \end{aligned} \quad (3)$$

where Θ refers to the Heaviside function, δ denotes the Kronecker symbol, the angled brackets $\langle \cdot \rangle$ signify the average taken over 100 trials with different initial conditions, and $N_{max} = 50000$ iteration steps is the length of the time series considered. Between the three h-quantities, the first two account for burst synchronization occurring when both of the neurons follow either the noninteracting (h_{00}) or the interacting map (h_{11}), whereas the "non-diagonal element" hnd covers the cases of the two neurons being synchronized while lying on the non-matching maps. Each of these terms may be linked with the paradigmatic time series and the accompanying phase plane diagrams, as shown in Fig. 2(b) and (c). Neglecting the "fine structure" behind the burst synchronization, we also determined the trial-averaged fraction of time the symbolic sequences of the two neurons overlap

$$H = \frac{1}{N_{max}} \left\langle \sum_{n=1}^{N_{max}} \delta_{S_{1,n},S_{2,n}} \right\rangle, \tag{4}$$

which amounts to the sum of the h-quantities. By definition, the spectra of H and h belong to the interval [0,1], so that their increase corresponds to improving burst synchronization. However, if H were to assume the upper-boundary value $H = 1$, this would not imply that the exact synchronization has been reached, though values less than *1* are sufficient to rule it out.

3. Results

Making use of the quantity H we were able to monitor the emergence and the succession of the regimes of burst synchronization in the (g_c, τ) space of the synaptic parameters. Since each point in this plane is associated with a specific type of waveforms, a first glance at the shading in Fig. 3 suggests that for an arbitrary g_c with increasing τ the antiphase synchronization gives way to the approximate synchronization in phase, this applying to both of the synaptic threshold behaviors.

A more detailed phase plane analysis tells us that the antiphase synchronization occurs by the lock-and-release mechanism [16,20], already recognized in case of the conductance-based neuron models. In brief, considering neurons 1 and 2, if 1 is bursting, $x_1 > \theta$ holds, so that the activated inhibitory synapse keeps the neuron 2 locked on the stable branch of the coupled map. In the next stage, as it ceases to burst, the neuron 1 releases from inhibition the neuron 2, that begins its own burst by switching to the isolated map, therefore pulling the neuron 1 to the stable branch of the coupled map. Comparing the small τ areas in Fig. 3(a) and (b), obtained for $k = 25$ and $k = 5$ respectively, it is possible to assert how "perfect" is the established regime of antiphase synchronization, or conversely, how often is the occurrence of accidental burst overlaps, depending on the gain parameter. As expected, the dynamics of the system for the FTM synapses turns out to be less irregular than the one for the graded synaptic transmission model.

Apart from the tendency to higher burst synchronization, what matters most about increasing τ is that there exist preferred g_c values where genuine in-phase synchronization is

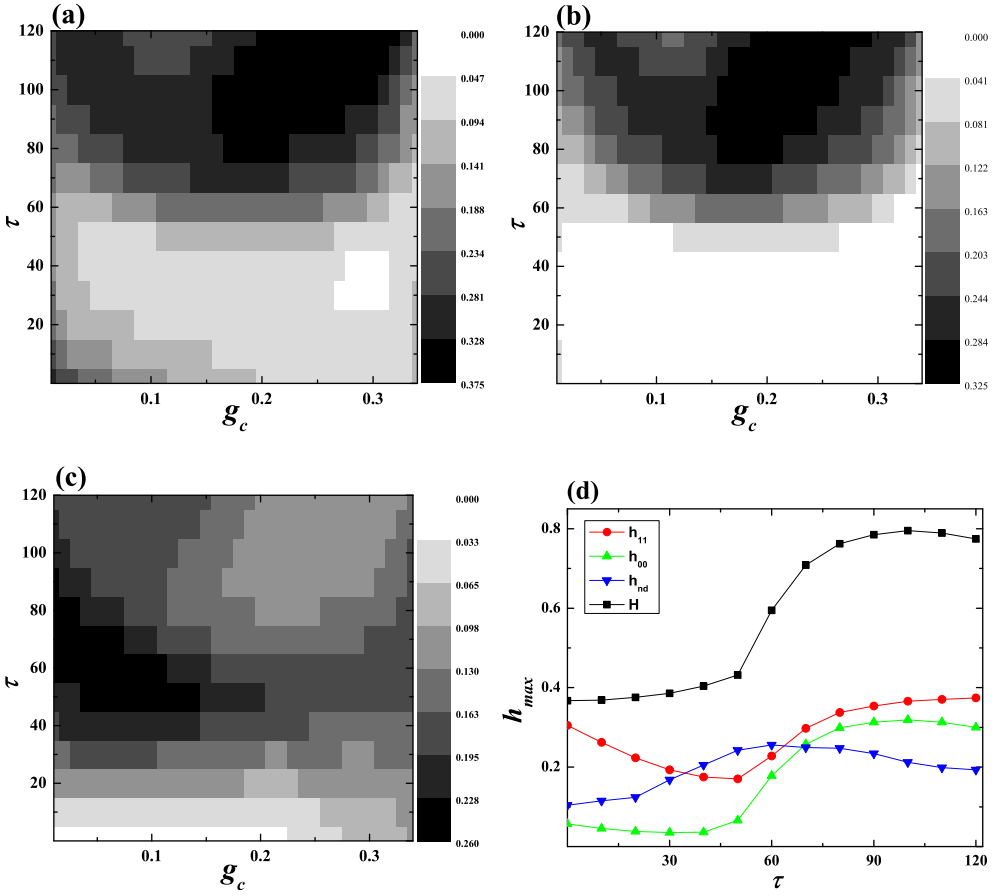

Fig. 4. (a), (b) and (c) Decomposition of H-synchronization into "elementary" terms, given by the h-quantities: h_{11} in (a), h_{00} in (b) and hnd in (c). The plots are displayed in the (g_c, τ) plane, keeping $k = 25$ fixed, with the darker shading representing the higher values. The small τ region in (b) shows the antiphase synchronization regime coinciding with the virtual absence of h_{00}. The high τ domains in (a) and (b), roughly matching the DMS, highlight the contribution to synchronization in phase by the h_{11} and h_{00} terms. (d) Dependence of H and h-quantities on τ, singled out by plotting the maximal values over g_c. The increase of h_{00} is seen essential in giving rise to burst synchronization with the synaptic delay.

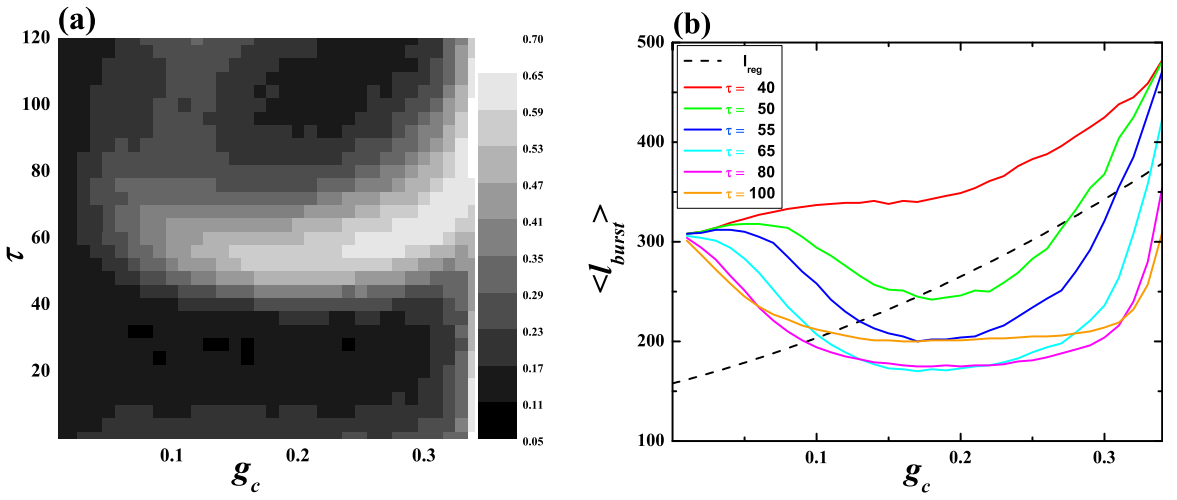

Fig. 5. (a) Regularity R dependence on g_c and τ: the lesser it becomes (darker shading), the more regular is the sequence of a neuron's burst cycles. From the small and high τ regions it is indicated that regularization accompanies mutual coordination, be it for the antiphase or the in-phase synchronization regime. (b) Family of curves displaying variation of the mean burst cycle $< l_{burst} >$ with g_c at fixed τ. In a dashed line is plotted an idealized burst cycle $l_{reg}(g_c) = 157.87 + 374.31 g_c + 808.2 g_c^2$, obtained neglecting the chaoticity and the effects of the synaptic delay, as if the bursts occurred exactly between the saddle-node point of the interacting map and the external crisis of the isolated map. Note that between $\tau \approx 50$ and $\tau \approx 65$, coinciding with the bright area in (a), the curves $< l_{burst} > (g_c)$ exhibit a sudden decrease, bending to intersect $l_{reg}(g_c)$ twice. For high τ, the reentrant point of intersection on the right is lost, as $< l_{burst} > (g_c)$ remain fairly constant over a considerable interval of weights.

achieved. This is preceded by a transitory area around $\tau \approx 60$ iteration steps, seen to coincide with the time series consisting of short and sparse synchronized bursts intermixed with the long desynchronized bursts, as remnants of the regime of antiphase synchronization. Moving further up, the H-synchronization, inhomogeneous with g_c, has a specific domain of maximal synchronization (DMS) standing out, that warrants the emergence of in-phase synchronization. It may seem curious that there is little to distinguish between the typical ways in which the in-phase and the antiphase synchronization are represented in the phase plane: for the former, the bursting also takes place on the isolated map, whereas the interburst intervals correspond to the motion along the stable branch of the coupled map, see Fig. 2(b). This is an immediate consequence of the synaptic delay: while neuron 1 is bursting, the openness of the synapse to neuron 2 is influenced by its preceding interburst interval and vice versa.

It is interesting that, enhancing τ, the orientation of the DMS depends on the gating behavior of the synapse: for higher (smaller) k, it is directed toward increasing (decreasing) g_c. The reverse orientation, along with the minor reduction of the level of synchronization, is caused by a lesser k endowing the presynaptic neuron with the ability to change the openness of the synapse in a continuous, rather than the discrete fashion, which can be interpreted in the phase plane as a slow drift of the effective interaction map. Put differently, the adjustment of bursting rhythms results from an interplay between the persistent influence of the synaptic parameters g_c and τ on one hand, and the k-dependent action of the presynaptic neuron potential, on the other. In the case of large k, the former is predominant, making it natural for the DMS to get shifted to higher g_c with the increase of τ. For small k, however, this is countered by the stronger impact of the presynaptic potential, causing the neurons to randomly fall out of step for overlong bursts, generated as the respective phase points "wander off" in the away area between the envelopes of the effective coupled map.

While so far we addressed the gross structure of the coordinated neuron activity, mirrored in the H-synchronization, we now look into the fine structure of burst synchronization, requiring that one determines the contribution each of the independent ("eigen") motif's dynamical configurations participates with in its establishment. In a broader sense, this is not unlike an attempt to expand the observed states of burst synchronization in terms of a complete set of vectors forming a basis. By the same token, the h-quantities, introduced in Section 2, present the probabilities for the neurons to lie in one of the synchronized states characterized by the respective motif's configuration. Proceeding along these lines, by making comparison between Fig. 4(a), (b) and (c), displaying h_{11}, h_{00} and hnd plots in the (g_c, τ) plane, one expects to gain more insight into the scenarios on how the emergence of different cooperative rhythms and their succession are realized.

In particular, from the small τ region in Fig. 4(b) we learn that the virtual absence of the h_{00} term plays a major part during the antiphase synchronization. On the other hand, this regime is compromised by the action of h_{11} and h_{nd}, where the latter, showing a steady increase consistent with the violation of the lock-and-release mechanism, appears decisive in its eventual breakdown. In fact, it is at the intermediate delays and for small weights that hnd reaches its maximal values, a detail we discuss further below. Turning to synchronization in phase, glancing the high τ regions in Fig. 4(a) and (b) reaffirms that h_{11} and h_{00}

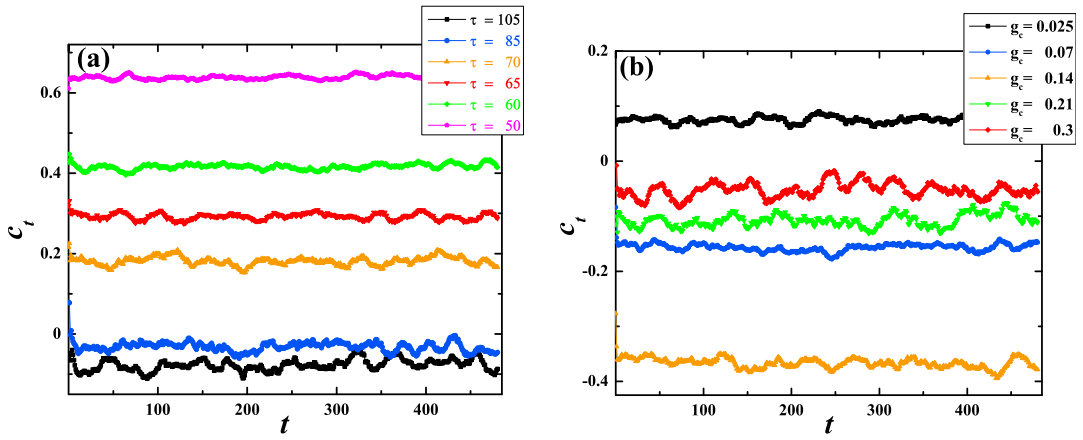

Fig. 6. (a) Family of c_t curves over τ for fixed $g_c = 0.23$. Along the decrease with the delay, note that the burst cycle deviations are highly correlated in the transitory area $\tau \in (50,65)$, whereas become virtually independent when synchronization in phase sets in ($\tau \geqslant 85$). (b) Family of c_t curves over g_c at $\tau = 100$. Approaching the DMS from the smaller weights, c_t reaches minimum around $g_c = 0.14$, regaining values close to *0* within and beyond the DMS. The minimum alone may reflect a kind of recovery mechanism, by which the deviations from periodic bursting are "repaired" through mutual adjustment of neuron activities.

contribute the regime in equal terms. In support of this, note that the darkest areas roughly match the DMS in Fig. 3, whereas the coincident *h*nd values remain very low, see Fig. 4(c). We summarize the aforementioned in Fig. 4(d), where the *h*-quantities dependence on τ is underlined by extracting their maximal values over g_c, viz. $h_{max}(\tau) = h_{max}(g_{c,max}(\tau), \tau)$. A point to be made is that the gain in burst synchronization with the synaptic delay is mostly due to the synchronization on the noninteracting maps, as witnessed by the nearly identical τ-coordinates of the inflection points in $H_{max}(\tau)$ and $h_{00,max}(\tau)$.

Before approaching the issue of collective neuron dynamics from another angle, let us examine whether there is periodicity in an individual neuron time series and determine how it is affected by the variation of the synaptic parameters. To this end, we consider the "regularity" quantity [31,32,26]

$$R = \frac{\sqrt{[< l^2 >] - [< l >]^2}}{[< l >]}, \tag{5}$$

assigning l to the duration of the burst cycle (time from the beginning of one burst to the beginning of the next), with the angled $\langle\cdot\rangle$ and squared brackets $[\cdot]$ denoting averages over a single trial and 100 different initial conditions, respectively. Given that R presents the normalized fluctuation of the burst cycle, its smaller values, displayed darker in Fig. 5(a), indicate the domains of synaptic parameters yielding higher regularity. Nonetheless, the highlight lies really in the general inference on the periodicity, maintained over the time series, being favorable to the establishment of the coordinated activity regimes, be it the antiphase or the in-phase synchronization of neurons.

As it turns out, within the entire (g_c, τ) plane, characterized by a tendency to periodic bursting, there is only a single island of irregularity, immersed around $\tau \approx 60$ and $g_c \gtrsim 0.12$. The reason for this behavior is implied by the Fig. 5(b), referring to the variation of the mean burst cycle (time and trial averaged) with g_c at fixed τ. Along with the family of curves obtained in a numerical simulation, we display for comparison what the plot of a hypothetical burst cycle l_{reg} (dashed line) would look like if the effects of the external crisis and the transmission delay were neglected. Crossing from the domain of antiphase synchronization into the intermediate τ region of high irregularity, not only do the curves exhibit a change in concavity, but are also seen to intersect $l_{reg}(g_c)$ twice. Hence, one may link the increase in R to a sudden reduction of the mean burst cycle. For τ above the transitory area, the curves remain virtually constant over a significant range of weights, giving rise to the eventual emergence of the in-phase synchronization. Finally, recalling what has been stated about the domain of maximal *h*nd following Fig. 4(c), we are now led to conclude that it coincides with the $\pi/2$ phase lag synchronization, as reflected in the interplay between the mean burst cycle and the synaptic delay, the latter being approximately 1/4 of the former.

After asserting the regularity for a broad range of synaptic parameters, we pursue the study of mutual adjustment between the two neurons' burst cycle sequences to probe how well are the deviations arising on one neuron matched by the cycle changes on the other. For this purpose, suppose that the durations of the corresponding burst cycles, l_1 and l_2, are sampled within the frames 4000 steps in width, and shifted by 200 steps relative to one another. Next, it is convenient to introduce the time dependent correlation coefficient

$$c_t = \frac{[< l_1 l_2 >_t] - [< l_1 >_t][< l_2 >_t]}{\sqrt{([< l_1^2 >_t] - [< l_1 >_t]^2)([< l_2^2 >_t] - [< l_2 >_t]^2)}}, \tag{6}$$

where t denotes the frame index, whereas the angled $\langle\cdot\rangle_t$ and the squared brackets $[\cdot]$ signify the averaging over the t-frame and 1000 different initial conditions. Here, $c_t \in [-1,1]$ holds, so that the upper (lower) boundary values indicate the deviations of one neuron's burst cycle countered by the deviations of the same (opposite) sign

on the other, while the values around 0 imply the deviations in the two sequences being independent.

We consider how c_t varies along the directions in the (g_c, τ) plane elaborately chosen to traverse the DMS. Fig. 6(a) shows a family of c_t curves over τ, obtained for fixed $g_c = 0.23$, beginning with the τ-values in the transitory area ($\tau = 50$), and ending deeply in the DMS ($\tau = 105$). One readily finds c_t decreasing with τ, a likely outcome of an emerging synchronization in phase due to an increase in the h_{00} term. Namely, at high τ, the cessation of bursts occurs on the isolated map, so that the deviations of the burst cycles remain independent. In the transitory area, however, we know there are opposing tendencies toward the antiphase and the in-phase synchronization giving rise to large fluctuations of the burst cycles (Fig. 5(a)), which now appear to be correlated. This is witnessed by the prevalence of the hnd term over h_{00} (Figs. 4(c) and (b)), that points to a majority of bursts terminated following the interacting map. In the next stage, we focus on the variation of c_t with g_c at fixed $\tau = 100$ (see the family of curves in Fig. 6(b)), along the path covering the motion from the slightly phase shifted burst synchronization, indicated by hnd > 0, to the proper synchronization in phase. One finds that c_t reduces to significantly negative values just before the DMS ($g_c = 0.14$), and then bounces back to the vicinity of 0. The negative c_t values imply the mutual adjustment and regulation between the sequences of the burst cycles involving a short-term "recovery mechanism" that may lie behind the observed periodicity in the neuron time series.

On a final note, we indicate how the introduced methods may be employed to study the effects of the parameter heterogeneity on burst synchronization taking the instances of the disparate stimulation currents and synaptic weights, the two cases likely to be encountered in real motifs [19]. For the former, comparing the $H(g_c, \tau)$ fields of a homogeneous and the inhomogeneous motif (not shown), one realizes that the stimuli heterogeneity is detrimental for the leading cooperative regime of activity, be it the antiphase or the in-phase synchronization. Picture becomes more interesting if there is a weight mismatch, as follows from the variation of the H field, $\Delta H(g_{c1}, g_{c2})$ with respect to g_{c2}, shown for the different values of τ in Fig. 7. Comparing Fig. 7(a), (b) and (c), the increase of τ is seen to induce greater order in the observed field, meaning that a more clear trend in the variation of H emerges in a larger domain of synaptic weights. Nonetheless, the values displayed in Fig. 7(b) and (c) also suggest for a higher delay to foster the growth of the portion in the (g_{c1}, g_{c2}) plane, where heterogeneity gives rise to burst synchronization.

4. Conclusions

In this contribution, instigated by the phase plane analysis, we have disclosed the fine structure of burst synchronization, a point reflected in the decomposition of the introduced quantity H over the h-terms, characterizing the action of the different dynamical configurations of the motif. The way the extracted subgraphs are assigned roles considering the observed non-linear phenomena is in direct relation to the nature of the synaptic model, whose threshold behavior is thought to faithfully reproduce the properties of interaction between real neurons. The h-quantity approach allows one to monitor in a continuous fashion the increase of burst synchronization with τ, in particular as to how and why the anti-phase synchronization is succeeded by the synchronization in phase. Another clue provided within this framework concerns a deeper insight into the regularization of neuron bursting, accompanying the emergence of both these regimes. However, though similar reasoning applied to the dependence of the burst cycle correlation on the synaptic parameters is sufficient to understand the ordering of the ensuing curves, the values alone are found indicative of the recovery mechanisms that make the neuron series robust against the violation of regularity.

Using the key points from above, we make an attempt to extend the argument into a field of research that remains slightly more tentative. Namely, thinking on a broader level, the presented analysis on how for a given structural motif one can determine the temporal evolution of the pertinent functional motifs may serve as a paradigm to characterize the succession of global emergent states by means of contributions from functional (effective) networks nested within the structural complex networks. For the latter, it has been demonstrated that models exist where synchronization is promoted through suppression of spatiotemporal chaos, if compared to regular or random networks. Along these lines, findings on the spatially

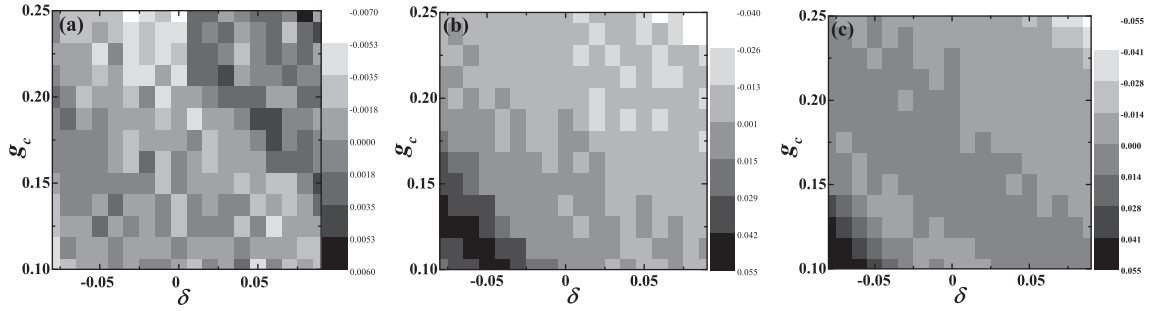

Fig. 7. Examining the effects of weight heterogeneity on H-synchronization. Letting the weights take values $g_{c1} = g_c$ and $g_{c2} = g_c + \delta$, we define the field of variation $\Delta H(g_c, \delta) = H(g_c, \delta) - H(g_c, \delta')$, where $\delta - \delta' = 0.01$ is the sampling step. The plots in (a), (b) and (c) are obtained for the delay values $\tau = 40$, 70 and 90, respectively. Unlike the chessboard-like appearance in (a), the enhanced order in (b) and (c) enables one to distinguish the heterogeneity effects more clearly. In particular, note that the increase of τ causes the band with the rising burst synchronization to expand.

extended networks of spiking neurons show that the fine tuning of the parameters such as synaptic delay, noise intensity or rewiring probability may lead to the appearance of waves and other spatiotemporal patterns of synchronized activity. This is upheld both in cases implementing the Rulkov map [33–36], and an array of conductance-based models, including Morris–Lecar [37], Fitzhugh–Nagumo [38] and Hodgkin–Huxley [39], some of the details contingent on whether the electrical or chemical synapses are applied [37,40].

A corollary of the collective neuronal dynamics, unfolding on a level of macroscopic structural network, is the perpetual change of the corresponding functional network, itself known to exhibit the properties of complex networks [4,5,41–43]. Observed within the short time windows, the fluctuations of the arising functional network turn out to be large, whereas for the sufficiently long time windows, with the fluctuations smoothed out,it is indicated how the structural and functional networks may show substantial overlap [41]. Nonetheless, considering the microscopic spatial scale, it may prove advantageous that the set of the obtained functional motifs could point to where the corresponding structural motif is situated. This reverse approach, in which the path to synchronization is employed to dissolve the structural networks into structural motifs, poses an issue already gaining interest in other areas, such as the systems of coupled Kuramoto oscillators [44].

Acknowledgement

This research was conducted under project No.171015, supported by the Serbian Ministry of Science and Technological Development.

References

[1] Milo R, Shen-Orr S, Itzkovitz S, Kashtan N, Chklovskii D, Alon U. Science 2002;298:824.
[2] Milo R, Itzkovitz S, Kashtan N, Levitt R, Shen-Orr S, Ayzenshtat I, et al. Science 2004;303:1538.
[3] Alon U. Nature 2007;8:450.
[4] Bullmore E, Sporns O. Nat Rev Neurosci. 2009;10:186.
[5] Sporns O, Chialvo DR, Kaiser M, Hilgetag CC. Trends Cogn Sci 2004;8:418.
[6] Sporns O, Kotter R. PLoS Biol 2004;2:e369.
[7] Song S, Sjostrom PJ, Reigl M, Nelson S, Chklovskii DB. PLoS Biol 2005;3:e68.
[8] Li C. Phys Rev E 2008;78:037101.
[9] Boccaletti S, Latora V, Moreno Y, Chavez M, Hwang DU. Phys Rep 2006;424:175.
[10] Nowotny T, Huerta R, Rabinovich MI. Chaos 2008;18:037119.
[11] Elson RC, Selverston AI, Huerta R, Rulkov NF, Rabinovich MI, Abarbanel HDI. Phys Rev Lett 1998;81:25.
[12] Elson RC, Selverston AI, Abarbanel HDI, Rabinovich MI. J Neurophysiol 2002;88:1166.
[13] Ibarz B, Cao H, Sanjuán MAF. Phys Rev E 2008;77:051918.
[14] Ivanchenko MV, Osipov GV, Shalfeev VD, Kurths J. Phys Rev Lett 2004;93:134101.
[15] Belykh I, de Lange E, Hasler M. Phys Rev Lett 2005;94:188101.
[16] Shilnikov A, Gordon R, Belykh I. Chaos 2008;18:037120.
[17] Franović I, Miljković V. Eur Phys J B 2010;76:613.
[18] Schimansky-Geier L, Anishchenko VS, Neiman A. In: Moss F, Gielen S, editors. Neuro-Informatics And Neural Modelling. Amsterdam: Elsevier; 2001.
[19] Belykh I, Shilnikov A. Phys Rev Lett 2008;101:078102.
[20] Koppel N, Ermentrout GB. In: Fiedler B, editor. Handbook Of Dynamical Systems. Amsterdam: Elsevier; 2002.
[21] Jalil S, Belykh I, Shilnikov A. Phys Rev E 2010;81:045201.
[22] Rulkov NF. Phys Rev Lett 2001;86:183.
[23] de Vries G. Phys Rev E 2001;64:051914.
[24] Innocenti G, Morelli A, Genesio R, Torcini A. Chaos 2007;17:043128.
[25] Burić N, Todorović K, Vasović N. Phys Rev E 2008;78:036211.
[26] Hilborn RC, Erwin RJ. Phys Rev E 2005;72:031112.
[27] Rowat PF, Selverston AI. J Comput Neurosci 1997;4:103.
[28] Somers D, Koppel N. Biol Cybernet 1993;68:393.
[29] Arbib MA, editor. Handbook Of Brain Theory And Neural Networks. Cambridge: MIT Press; 2003. p. 47.
[30] Varona P, Torres JJ, Huerta R, Abarbanel HDI, Rabinovich MI. Neural Netw 2001;14:865.
[31] Pikovsky AS, Kurths J. Phys Rev Lett 1997;78:775.
[32] Guo D, Li C. Phys Rev E 2009;79:051921.
[33] Wang Q, Duan Z, Perc M, Chen G. EPL 2008;83:50008.
[34] Wang Q, Perc M, Duan Z, Chen G. Phys Rev E 2009;80:026206.
[35] Perc M. Phys Rev E 2007;76:066203.
[36] Perc M. Chaos Soliton Fract 2007;31:64.
[37] Wang Q, Perc M, Duan Z, Chen G. Phys A 2010;389:3299.
[38] Kwon O, Jo HH, Moon HT. Phys Rev E 2005;72:066121.
[39] Kwon O, Moon HT. Phys Lett A 2002;298:319.
[40] Perc M. Biophys Chem 2009;141:175.
[41] Honey CJ, Kötter R, Breakspear M, Sporns O. PNAS 2007;104:10240.
[42] Eguíluz VM, Chialvo DR, Cecchi GA, Baliki M, Apkarian AV. Phys Rev Lett 2005;94:018102.
[43] Zhou C, Zemanová L, Zamora G, Hilgetag CC, Kurths J. Phys Rev Lett 2006;97:238103.
[44] Arenas A, Díaz-Guilera A, Pérez-Vicente CJ. Phys Rev Lett 2006;96:114102.